Available online at www.sciencedirect.com
ScienceDirect
Journal of Solid State Chemistry 180 (2007) 2225–2232
JOURNAL OF SOLID STATE CHEMISTRY
www.elsevier.com/locate/jssc

Synthesis and structure of a 1,6-hexyldiamine heptaborate, $[H_3N(CH_2)_6NH_3][B_7O_{10}(OH)_3]$

Sihai Yang[a], Guobao Li[a,*], Shujian Tian[a], Fuhui Liao[a], Ming Xiong[b], Jianhua Lin[a]

[a]*Beijing National Laboratory for Molecular Sciences (BNLMS), State Key Laboratory of Rare Earth Materials Chemistry and Applications, College of Chemistry and Molecular Engineering, Peking University, Beijing 100871, PR China*
[b]*China University of Geoscience, X-ray Laboratory, Beijing 100083, PR China*

Received 13 March 2007; received in revised form 14 May 2007; accepted 30 May 2007
Available online 6 June 2007

Abstract

A new 1,6-hexyldiamine heptaborate, $[H_3N(CH_2)_6NH_3][B_7O_{10}(OH)_3]$ (**1**), has been solvothermally synthesized and characterized by single-crystal X-ray diffraction, FTIR, elemental analysis, and thermogravimetric analysis. Compound **1** crystallizes in monoclinic system, space group $P2_1/n$ with $a = 8.042(2)$ Å, $b = 20.004(4)$ Å, $c = 10.103(2)$ Å, and $\beta = 90.42(3)°$. The anionic $[B_7O_{10}(OH)_3]_n^{2n-}$ layers are interlinked via hydrogen bonding to form a 3D supramolecular network containing large channels, in which the templated $[H_3N(CH_2)_6NH_3]^{2+}$ cations are located.

Keywords: Polyborate; Heptaborate; Solvothermal reaction; Structure; Space group $P2_1/n$; Supramolecular

1. Introduction

Borates have been widely studied due to their rich structural chemistry [1–5] and potential applications in UV laser and nonlinear optical materials [6–8]. These compounds are usually composed of hydrated or anhydrous borate polyanions and metal ions, such as alkali ion [9], alkaline earth ion [10], transition metal ion [2,5], rare earth ion [11], main group metal ion [12–14] or metal complex ions [15]. Recently, several porous borates [2–5,16] have been reported with a small template or without any template, which induces a strong interest in such a kind of material. Because the nonmetal cation, such as 1,6-hexyldiamine, can be a large template, many studies have been focused on the nonmetal cation-templated borates [15,17–21]. Most of the reported organic template borates consist of isolated polyanions such as $[B_5O_6(OH)_4]^-$ [17,18] $[B_8O_{10}(OH)_6]^{2-}$ [17], $[B_9O_{12}(OH)_6]^{3-}$ [19] and $[B_{14}O_{20}(OH)_6]^{4-}$ [20]. However, the two-dimensional organically templated borates are rare to see, with few examples such as $[NH_3CH_2CH_2NH_3][B_6O_9(OH)_2]$ [22]. During our study on porous borate templated by nonmetal cation, a novel organically templated-layered borate $[H_3N(CH_2)_6NH_3][B_7O_{10}(OH)_3]$ (**1**) has been solvothermally synthesized. Here, the synthesis, structure and thermal property of **1** are presented.

2. Experimental

2.1. Materials and analyses

All reagents were of analytical grade and were used as obtained from commercial sources without further purification. The products were examined by X-ray diffraction on a Rigaku D/Max-2000 diffractometer with graphite monochromatized Cu$K\alpha$ radiation. IR spectra were recorded in the 400–4000 cm^{-1} range using a Magna-IR 750 FTIR spectrometer. ^{11}B solid-state NMR spectrum was recorded on a Varian Unity Plus-400 spectrometer. The recording conditions of the spectrum are listed in Table 1. Elemental analyses were carried out on Elementar Vario EL III microanalyzer. Thermogravimetric–mass spectrometric analysis (TG–MS) was performed in a Netzsch STA 449C simultaneous analyzer utilizing Al_2O_3 crucibles and type-S thermocouples. The thermal stability was investigated up to 1073 K with TG–MS in a heating/

---

*Corresponding author. Fax: +86 10 62753541.
E-mail address: liguobao@pku.edu.cn (G. Li).

0022-4596/$ - see front matter © 2007 Elsevier Inc. All rights reserved.
doi:10.1016/j.jssc.2007.05.029

Table 1
Recording conditions of the CPMAS NMR spectrum of ^{11}B

Chemical shift standard	$BF_3 \cdot OEt_2$
Frequency (MHz)	128.2503
Pulse width (μs)	0.3
Flip angle	$\pi/10$
Recycle time (s)	8
Spinning rate (kHz)	20
Number of scans	91

Table 2
Crystallographic and structure refinement parameters for **1**

Formula	$[H_3N(CH_2)_6NH_3][B_7O_{10}(OH)_3]$
f_w	404.92
Crystal system	Monoclinic
Space group	$P2_1/n$
a (Å)	8.042(2)
b (Å)	20.004(4)
c (Å)	10.103(2)
β	90.42(3)°
V (Å^3)	1625.3(6)
Z	4
$d_{calcd.}$ (g cm^{-3})	1.655
T (K)	298
λ (Mo$K\alpha$) (Å)	0.71073
μ (mm^{-1})	0.145
$R_1(I>2\delta(I))$[a]	0.0636
wR_2 (all data)[a]	0.1529

[a] $R_1 = \sum(||F_0| - |F_c||)/\sum|F_0|$. $wR_2 = [\sum(F_0^2 - F_c^2)^2/\sum(F_0^2)^2]^{1/2}$. $w = 1/[\sigma^2(F_0^2) + (0.0518P)^2 + 1.8800P]$, where $P = (F_0^2 + 2F_c^2)/3$.

cooling rate of 10 K/min in dynamic argon atmosphere (gas flow 0.03 L/min).

2.2. Preparation of $[H_3N(CH_2)_6NH_3][B_7O_{10}(OH)_3]$

$[H_3N(CH_2)_6NH_3][B_7O_{10}(OH)_3]$ was synthesized by the solvothermal method. A 50 mL Teflon autoclave was loaded with a mixture of H_3BO_3 (12.0 g, 194.1 mmol), $H_2N(CH_2)_6NH_2$ (6.0 g, 50.8 mmol) and C_2H_5OH (15.0 mL, 0.26 mol) with a mole ratio of 3.8:1.0:5.1, heated at 150 °C for 5 days, and then cooled to room temperature at a rate of 5 °C/h. After the solvothermal treatment, colorless needle-like crystals were obtained, filtered, washed with distilled water and ethanol, and isolated in ca. 90% initial yield (based on H_3BO_3). These colorless crystals cannot dissolve in water and most organic solvents. Anal. calcd. for **1**: C, 17.80% N, 6.92% H, 5.23%. Found: C, 18.01% N, 6.94% H, 5.33%.

2.3. Crystallographic studies

A single crystal of **1** (colorless, dimensions $0.2 \times 0.1 \times 0.1\,mm^3$) was carefully selected under an optical microscope and glued to a thin glass fiber with epoxy resin. Intensity data were collected on a Bruker SMART X-ray diffractometer, equipped with an APEX-CCD area detector and using graphite-monochromated Mo$K\alpha$ ($\lambda = 0.71073$ Å) radiation at room temperature. The data

Table 3
Atomic parameters of $[H_3N(CH_2)_6NH_3][B_7O_{10}(OH)_3]$

Atom	x	y	z	Atom	x	y	z
B1	1.2096(2)	0.2914(1)	0.2558(2)	H1C	0.5794	0.1898	0.0359
B2	1.0140(2)	0.2112(1)	0.1218(2)	C2A[a]	0.5674(4)	0.0972(1)	0.1024(3)
B3	0.9387(2)	0.2493(1)	0.3454(2)	H2A	0.4544	0.0848	0.0791
B4	1.2090(2)	0.2949(1)	−0.0072(2)	H2B	0.6428	0.0832	0.0332
B5	0.9542(2)	0.2506(1)	−0.1095(2)	C2B[a]	0.5147(2)	0.1058(7)	0.1551(1)
B6	1.0763(3)	0.0887(1)	0.0829(2)	C3	0.6132(5)	0.0629(2)	0.2261(3)
B7	1.2759(3)	0.3939(1)	0.1340(2)	H3A	0.5304	0.0639	0.2955
O1	0.9245(2)	0.2093(1)	−0.0035(1)	H3B	0.7147	0.0832	0.2594
O2	1.1364(1)	0.2685(1)	0.1231(1)	C4	0.6385(5)	−0.0099(1)	0.2231(3)
O3	1.0874(2)	0.2812(1)	0.3574(1)	H4A	0.7188	−0.0202	0.1549
O4	1.0791(2)	0.2961(1)	−0.1057(1)	H4B	0.5343	−0.0310	0.1981
O5	0.8951(2)	0.2191(1)	0.2287(1)	C5	0.6970(5)	−0.0396(1)	0.3492(3)
O6	1.2707(2)	0.3630(1)	0.0144(1)	H5A	0.7863	−0.0115	0.3824
O7	1.1043(2)	0.1473(1)	0.1450(1)	H5B	0.6116	−0.0166	0.3989
O8	1.3585(2)	0.2517(1)	0.2794(1)	C6A[b]	0.7579(5)	−0.1089(2)	0.3519(3)
O9	0.8451(2)	0.2485(1)	0.4563(1)	H6A	0.6767	−0.1362	0.3055
O10	1.2471(2)	0.3625(1)	0.2494(1)	H6B	0.8627	−0.1112	0.3051
O11	0.9780(2)	0.0801(1)	−0.0274(2)	C6B[b]	0.6711(2)	−0.1021(7)	0.4018(2)
H11	0.9538	0.1167	−0.0586	C7	0.7822(4)	−0.1393(1)	0.4833(3)
O12	1.1493(2)	0.0319(1)	0.1340(2)	H7A	0.8233	−0.1844	0.4709
H12	1.1325	−0.0010	0.0875	H7B	0.7155	−0.1425	0.5627
O13	1.3215(2)	0.4606(1)	0.1324(2)	N8	0.9006(2)	−0.1038(1)	0.5746(2)
H13	1.3200	0.4755	0.2080	H8A	0.8762	−0.0605	0.5762
N1	0.5744(2)	0.1715(1)	0.1160(2)	H8B	1.0041	−0.1093	0.5459
H1A	0.6648	0.1827	0.1623	H8C	0.8919	−0.1207	0.6557
H1B	0.4845	0.1863	0.1575	–	–	–	–

[a] The occupation ratio for C2A:C2B is 0.85:0.15.

[b] The occupation ratio for C6A:C6B is 0.85:0.15.

Table 4
Selected bond distances (Å) for $[H_3N(CH_2)_6NH_3][B_7O_{10}(OH)_3]$

B1–O3	1.441(2)	B3–O3	1.360(2)	B6–O7	1.347(2)	C2B–C3	1.368(16)
B1–O8	1.454(2)	B3–O5	1.368(2)	B6–O11	1.372(3)	C3–C4	1.470(4)
B1–O10	1.456(2)	B4–O4	1.438(2)	B6–O12	1.377(2)	C4–C5	1.479(4)
B1–O2	1.530(2)	B4–O9[#1]	1.446(2)	B7–O10	1.346(2)	C5–C6B	1.376(15)
B2–O1	1.452(2)	B4–O6	1.467(2)	B7–O6	1.357(2)	C5–C6A	1.470(4)
B2–O5	1.457(2)	B4–O2	1.537(2)	B7–O13	1.384(2)	C6A–C7	1.472(4)
B2–O7	1.488(2)	B5–O4	1.355(2)	N1–C2B	1.453(14)	C6B–C7	1.420(16)
B2–O2	1.511(2)	B5–O8[#2]	1.357(2)	N1–C2A	1.493(3)	C7–N8	1.499(3)
B3–O9	1.354(2)	B5–O1	1.375(2)	C2A–C3	1.471(4)		

Symmetry transformations used to generate equivalent atoms: [#1] $x+1/2, -y+1/2, z-1/2$; [#2] $x-1/2, -y+1/2, z-1/2$.

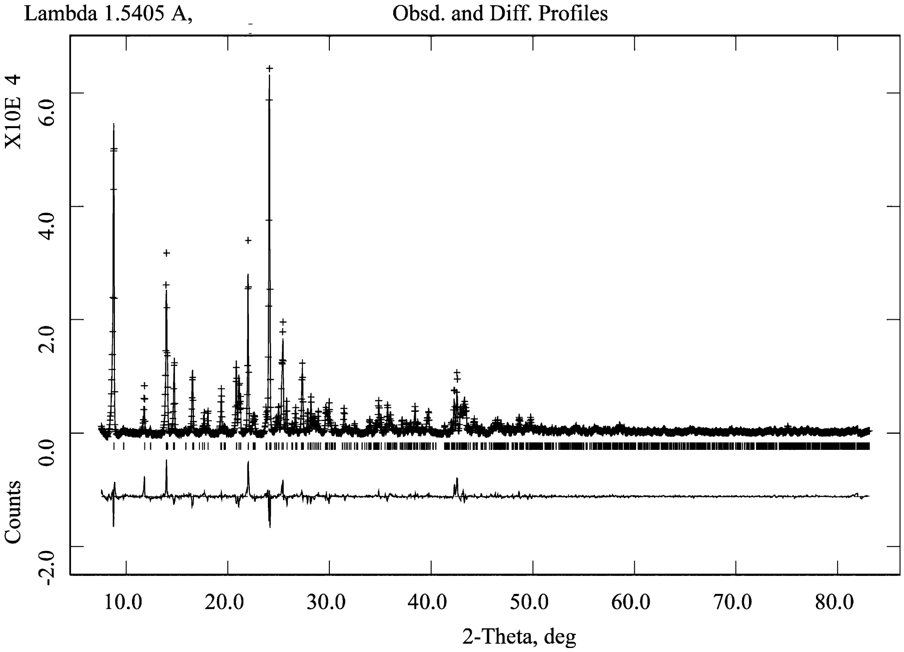

Fig. 1. Rietveld plots of the X-ray diffraction patterns of **1**. The symbol (+) represents the observed value, solid line represents the calculated value; the marks below the diffraction patterns are the calculated reflection positions, and the difference curve is shown at the bottom of the figure.

absorption correction was applied based on symmetry-equivalent reflections using the ABSOR program [23]. The structure was solved with direct methods and refined on F^2 with full-matrix least-squares methods using SHELXS-97 and SHELXL-97 programs, respectively [24,25]. All non-hydrogen atoms were refined anisotropically. The hydrogen atoms were added in the riding model and refined isotropically with O–H = 0.82 Å, C–H = 0.97 Å (for CH_2 group) and N–H = 0.89 Å. In the region of the $[H_3N(CH_2)_6NH_3]^{2+}$ cation, the difference electron density map showed two electron density features separated by a short distance (about 1 Å), and two H atoms are located nearby. As a result, we found one disordered C atom (C2) with a ca. 0.85:0.15 occupancy ratio for its C2A and C2B components; similarly, we identified another disordered C atom (C6), with a similar occupancy ratio for C6A and C6B. The crystallographic data for **1** are summarized in Table 2, and the atomic parameters and the selected bond lengths are listed in Tables 3 and 4, respectively. Crystallographic data (excluding structure factors) for the structure reported in this paper have been deposited with the Cambridge Crystallographic Data Centre as supplementary publication no. CCDC 637209. Copies of the data can be obtained free of charge on application to CCDC, 12 Union Road, Cambridge CB2 1EZ, UK (fax: +44 1223 336 033; e-mail: deposit@ccdc.cam.ac.uk). In order to check the phase purity of the sample in large scale, the X-ray diffraction patterns of the powder sample of **1** for structure refinement were recorded on a Bruker D8 Advance diffractometer with Cu$K\alpha_1$ ($\lambda = 1.54056$ Å) radiation (2θ range: 8–80°; step: 0.0144°; scan speed: 40 s/step) at 50 kV and 40 mA at room temperature as shown in Fig. 1, which fitted well with $R_p = 0.035$ and $R_{wp} = 0.051$ using GSAS software [26] by

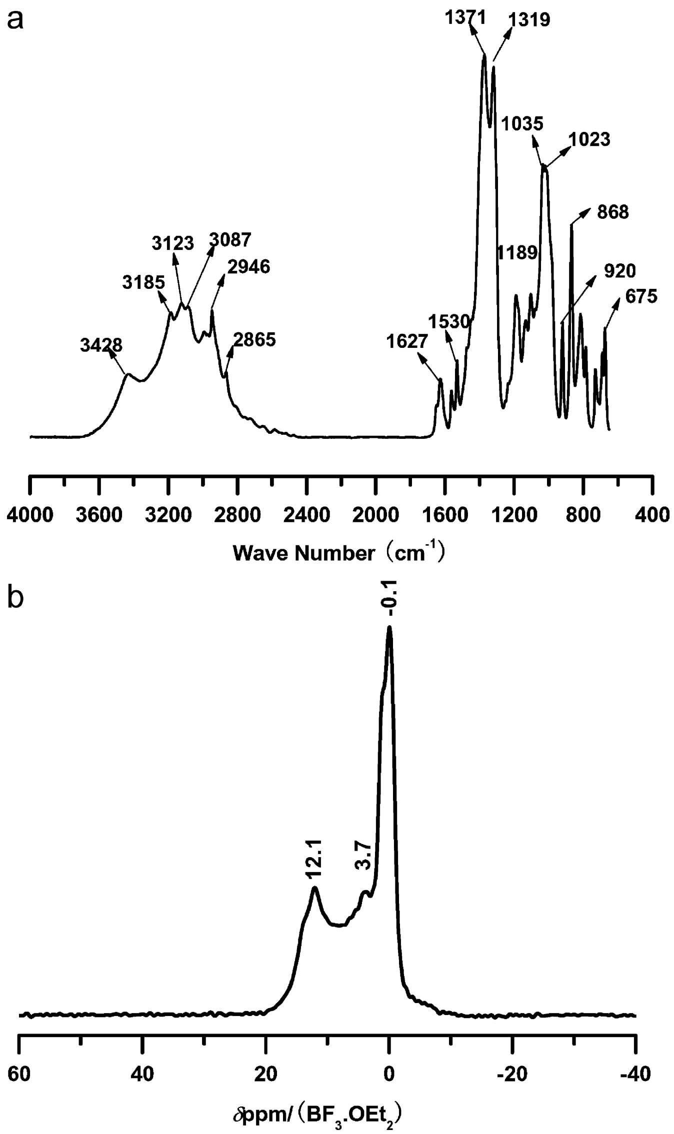

Fig. 2. IR spectrum and CPMAS NMR spectrum of ^{11}B for $[H_3N(CH_2)_6NH_3][B_7O_{10}(OH)_3]$.

Rietveld method [27] to confirm that the pure sample can be obtained in large scale. During the Rietveld refinement of the powder X-ray diffraction data, the crystallographic data listed in Table 2 and the atomic parameters listed in Table 3 were used and kept unchangeable, the parameters to be refined were just background coefficients, diffractometer constants, profile coefficients and preferred orientation parameters [26].

3. Results and discussion

3.1. Infrared (IR) spectra and solid-state CPMAS NMR spectra

The IR spectrum and the CPMAS NMR spectrum of ^{11}B for **1** are shown in Fig. 2. The recorded FTIR spectrum was compared with the standard spectrum of the functional groups. The stretching vibrations of the O–H, N–H, and C–H bands are observed at ~3428, 3185, 3123, 2946, and 2865 cm^{-1}. The strong bands at ~1371, 1319, 920, and 675 cm^{-1} in the spectra are characteristic of BO_3 [28], while the bands around 1035, 1023, and 868 cm^{-1} are characteristic of BO_4 [28], and the stretching vibrations of the C–N band are also located around 1189 cm^{-1}. The broad peaks around 12.1 and 3.37 ppm in the CPMAS NMR spectrum of ^{11}B for **1** (Fig. 2b) are assigned to the ^{11}B atoms in the BO_3 groups, which are affected by second-order quadrupolar broadening effects. In addition, the sharp peaks around −0.1 ppm are for the ^{11}B atoms in the BO_4 groups, for which second-order quadrupolar effects are absent owing to its more symmetric local environment. These values agreed well with the reported ones [29–31].

3.2. Crystal structure

There are one $[H_3N(CH_2)_6NH_3]^{2+}$ cation and one fundamental building block (FBB) of $[B_7O_{12}(OH)_3]^{6-}$ in an asymmetric unit of $[H_3N(CH_2)_6NH_3][B_7O_{10}(OH)_3]$ (see Fig. 3). The structure refinement clearly indicated that the $[H_3N(CH_2)_6NH_3]^{2+}$ cation contains two sets of disordered carbon atoms, C2A, C2B and C6A, C6B with occupation of 0.85 (C2A and C6A) and 0.15 (C2B and C6B), respectively, as shown in Fig. 3b. The FBB of $[B_7O_{12}(OH)_3]^{6-}$ consists of 7 B atoms, 3 OH groups and 12 oxygen atoms to form a $[B_6O_{12}(OH)]$ unit (noted as $3\geqslant+3T$) and a $[BO(OH)_2]$ unit (as $1\geqslant$) [32,33]. The $[B_6O_{12}(OH)]$ unit is a three-joint three-membered ring containing an unusual O atom bonded to three boron atoms. A similar borate unit has been reported in several known borates, such as tunellite [34], strontioborite [35], $Ln[B_8O_{11}(OH)_5]$ (Ln = La–Nd) [11] and $Ln[B_9O_{13}(OH)_4]\cdot H_2O$ (Ln = Pr–Eu) [11]. As it is known, there are many different FBBs for the heptaborates, and Fig. 4 shows several samples of them. The FBB shown in Fig. 4a is for $Na_3B_7O_{12}$ [36], which consists of three groups, B_3O_7, BO_3 and B_3O_8, connected by corner sharing. Such a FBB is also found in $Li_3B_7O_{12}$ [37]. The FBB shown in Fig. 4b is found in several compounds, such as $Cs_2[B_7O_9(OH)_5]$ [38], $[Cu(en)_2][B_7O_{10}(OH)_3]$ (en = ethylenediamine) [39], $[H_2DAB][B_7O_9(OH)_5]\cdot 2H_2O$ and $[H_2DAB][B_7O_{10}(OH)_3]$ (DAB = 1,4-diaminobutane) [40]. It is very similar to the FBB shown in Fig. 4a using a B_3O_7 group and not the B_3O_8 group. There are few compounds to have the FBB shown in Fig. 4(c–e), which consist of a B_7O_{14} group, a B_5O_{12} group and two BO_4 groups, and a B_3O_8 group and four BO_3 groups, respectively. The FBB shown in Fig. 4f is for $Ni_3B_7O_{13}Br$ [43], which consists of a BO_3 group and a B_6O_{16} group formed by three B_3O_9 groups using edge sharing. This FBB is common for the orthorhombic boracite-type compounds with the formula M3B7O13X (M = Mg, Fe, Co, Ni, Cu; X = Cl, Br, I), which is very similar to that for $[H_3N(CH_2)_6NH_3][B_7O_{10}(OH)_3]$. The B_6O_{16} group in $Ni_3B_7O_{13}Br$ is changed to the B_6O_{13} group

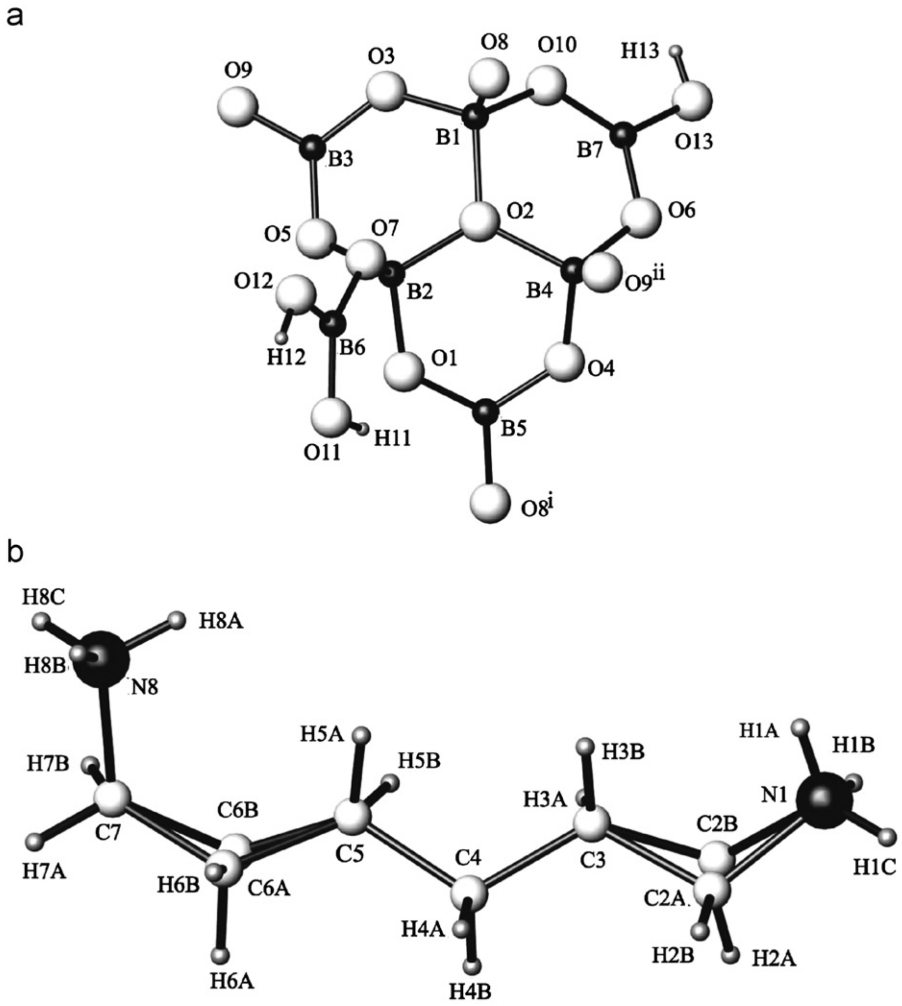

Fig. 3. Structure descriptions of $[H_3N(CH_2)_6NH_3][B_7O_{10}(OH)_3]$: (a) $[B_7O_{12}(OH)_3]^{6-}$; (b) $[H_3N(CH_2)_6NH_3]^{2+}$ with the disordered C atoms, the hydrogen atoms on C2B and C6B were not added. Symmetry codes: (i) $x-1/2$, $-y+1/2$, $z-1/2$; (ii) $x+1/2$, $-y+1/2$, $z-1/2$.

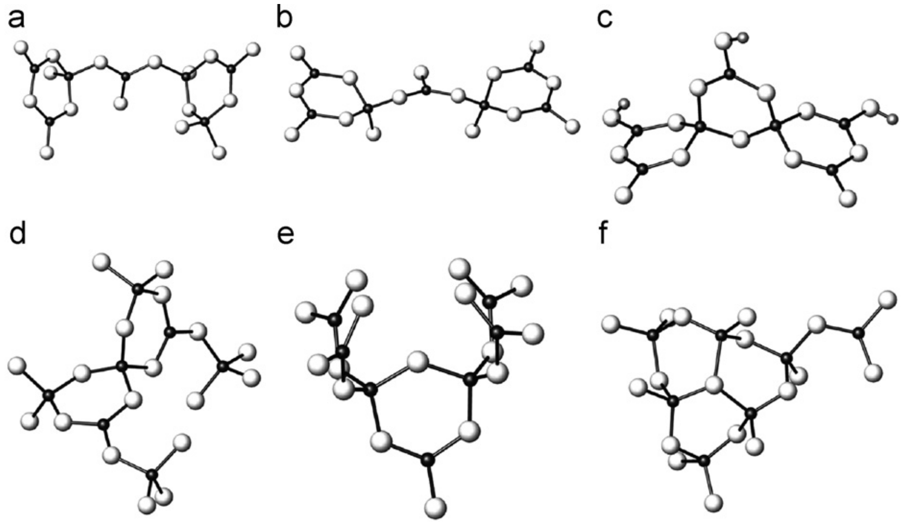

Fig. 4. FBB of the compounds $Na_3B_7O_{12}$ [36] (a), $Cs_2[B_7O_9(OH)_5]$ [38] (b), $M\mathrm{CuB_7O_{12}}\cdot n\mathrm{H_2O}$ (M = Na, K) [5] (c), $NaBa_3Si_2B_7O_{16}(OH)_4$ (d) [41], $K_3[Pt(B_7O_{11}(OH)_5)(OH)]\cdot 3H_2O$ (e) [42], and $Ni_3B_7O_{13}Br$ (f) [43]. FBBs of the reported heptaborates: oxygen, white circle; boron, black circle.

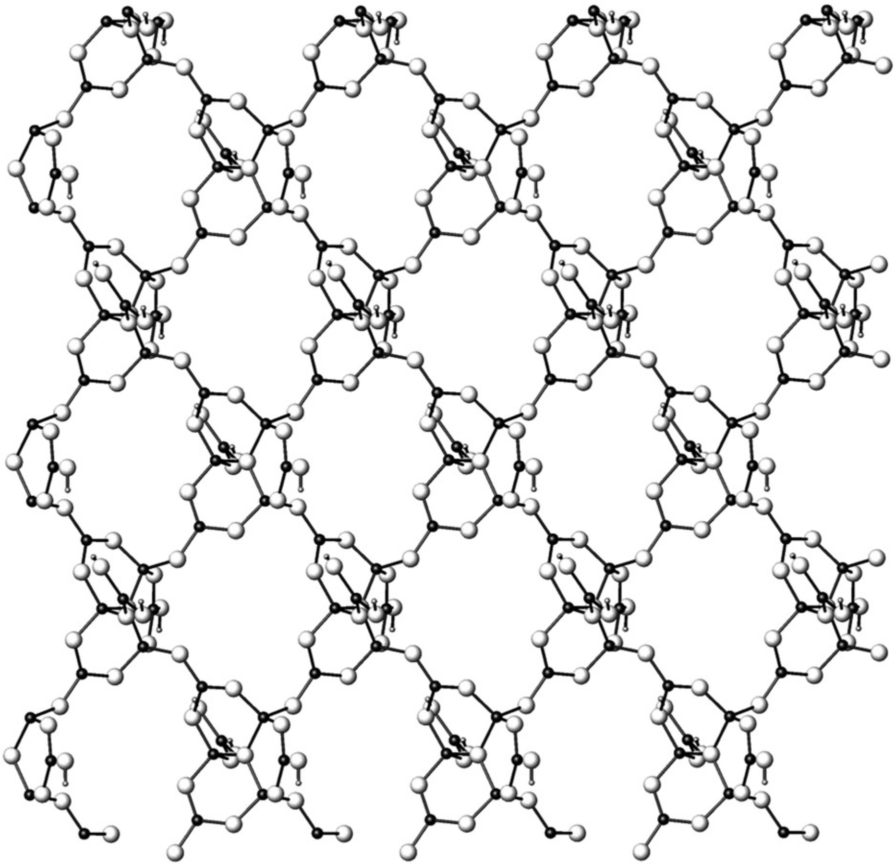

Fig. 5. The projection of the layer $[B_7O_{10}(OH)_3]_n^{2n-}$ viewed along *b*-axis.

in $[H_3N(CH_2)_6NH_3][B_7O_{10}(OH)_3]$, which is formed by three B_3O_8 groups with edge sharing. It is needed to mention that only a few of types of FBB with seven boron atoms are shown in Fig. 4, in which it is difficult and not necessary to present all the types. For example, the FBB of $AgSrB_7O_{12}$ [44] consists of one B_3O_8 group, two BO_3 groups and two BO_4 groups. In addition, several so-called heptaborates do not consist of the FBB with only seven boron atoms, such as $Cs_3B_7O_{12}$ [45] and the cubic boracite $CrB_7O_{13}Cl$ [46].

There are three terminal OH group (O11H11, O12H12 and O13H13) and four terminal oxygen atoms (O8, O9, $O8^{i}$, and $O9^{ii}$) in the FBB of $[B_7O_{12}(OH)_3]^{6-}$. With the help of the terminal oxygen atoms, the units $[B_7O_{12}(OH)_3]^{6-}$ link to each other to form a layer $[B_7O_{10}(OH)_3]_n^{2n-}$ as shown in Fig. 5. In that case, this hydrated heptaborate can be described as borate layers that stack one over another, forming the polyborate structure. When seen along the *b*-axis, the layers $[B_7O_{10}(OH)_3]_n^{2n-}$ contain vacancies formed by nine-member rings, which consist of four units of $[B_7O_{12}(OH)_3]^{6-}$. On the other hand, seen along the *c*-axis, it is found that the branches $[BO(OH)_2]$ point to both sides of the primary borate layer alternately, which lead to zig-zag deformation of the primary borate layer.

Although the borate framework in **1** is two dimensional, the $[B_7O_{10}(OH)_3]_n^{2n-}$ layers connect to each other by extensive hydrogen bonding to form a three-dimensional network as shown in Fig. 6. Large cavities can be observed along the *c*-axis (Fig. 6a), and they are filled with the template cations $[H_3N(CH_2)_6NH_3]^{2+}$ as shown Fig. 6b. The cavities, seen from the *b*-axis, are filled with the terminal groups $\text{-}NH_3^+$, which are linked to the layer $[B_7O_{10}(OH)_3]_n^{2n-}$ by hydrogen bonding listed in Table 5.

3.3. Thermal properties

As shown in Fig. 7, the TG curve of **1** showed that the compound was stable up to about 291 °C, then a continuous weight loss occurred between 291 and 550 °C, corresponding to the removal of one $H_2N(CH_2)_6NH_2$, and two-and-half water molecules from the dehydration of hydroxyls (found: 40.6%; calcd.: 39.8%). The powder X-ray diffraction data of **1** treated at different temperatures show that the structure does not decompose up to 290 °C, and when the temperature is up to 310 °C only the strong diffraction patterns can be observed, indicating that the compound **1** is not stable at this temperature (Fig. 8).

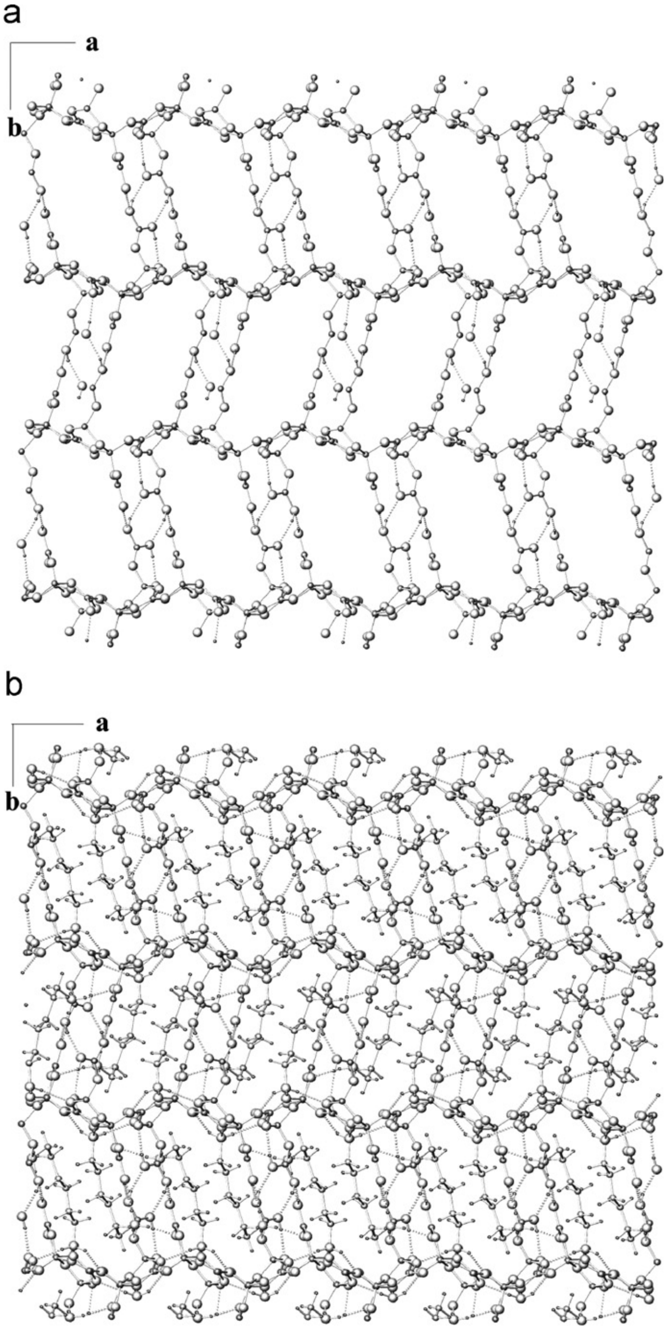

Fig. 6. The projection of the compound $[H_3N(CH_2)_6NH_3][B_7O_{10}(OH)_3]$: (a) along the *c*-axis without $[H_3N(CH_2)_6NH_3]^{2+}$; (b) along the *c*-axis with $[H_3N(CH_2)_6NH_3]^{2+}$.

4. Conclusion

A layered 1,6-hexyldiamine heptaborate, $[H_3N(CH_2)_6NH_3][B_7O_{10}(OH)_3]$, was solvothermally synthesized at 150 °C. It crystallized in monoclinic space group $P2_1/n$ with $a = 8.042(2)$ Å, $b = 20.004(4)$ Å, $c = 10.103(2)$ Å, and $\beta = 90.42(3)^\circ$. It consists of the layers $[B_7O_{10}(OH)_3]_n^{2n-}$ and the counter ions $[H_3N(CH_2)_6NH_3]^{2+}$. This compound started to decompose at about 290 °C.

Table 5
Details of hydrogen bonds for $[H_3N(CH_2)_6NH_3][B_7O_{10}(OH)_3]$

D–H···A	D–H (Å)	H···A (Å)	D–H···A (Å)
O11–H11···O1	0.82	1.95	2.631(2)
O12–H12···O11[#1]	0.82	1.91	2.686(2)
O13–H13···O12[#2]	0.82	1.97	2.767(2)
N1–H1A···O5	0.89	2.10	2.969(2)
N1–H1B···O8[#3]	0.89	2.07	2.891(2)
N1–H1C···O3[#4]	0.89	1.90	2.782(2)
N8–H8A···O13[#5]	0.89	2.12	2.994(2)
N8–H8B···O6[#6]	0.89	1.99	2.876(2)
N8–H8C···O7[#7]	0.89	2.08	2.965(2)

Symmetry transformations used to generate equivalent atoms: [#1] $2-x, -y, -z$; [#2] $-x+5/2, y+1/2, -z+1/2$; [#3] $x-1, y, z$; [#4] $x-1/2, -y+1/2, z-1/2$; [#5] $x-1/2, -y+1/2, z+1/2$; [#6] $-x+5/2, y-1/2, -z+1/2$; [#7] $-x+2, -y, -z+1$.

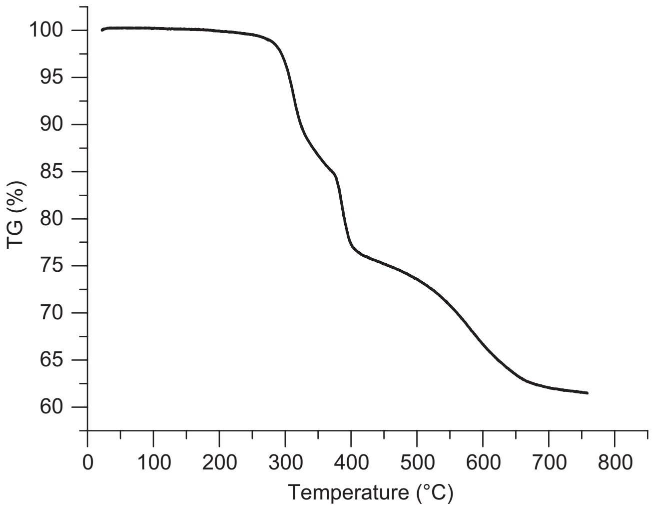

Fig. 7. TG curves for $[H_3N(CH_2)_6NH_3][B_7O_{10}(OH)_3]$.

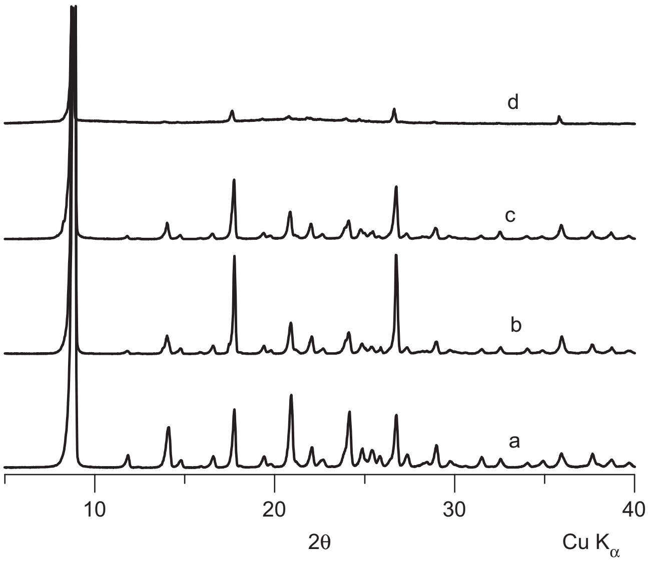

Fig. 8. X-ray diffraction patterns of $[H_3N(CH_2)_6NH_3][B_7O_{10}(OH)_3]$ treated at different temperatures: (a) $[H_3N(CH_2)_6NH_3][B_7O_{10}(OH)_3]$ as obtained (referred as Sample A), (b) heating Sample A at 260 °C for 12 h (Sample B), (c) heating Sample B at 290 °C for 12 h (Sample C), (d) heating Sample C at 310 °C for 12 h (Sample D).

Acknowledgment

This work is supported by the National Natural Science Foundation of China (Grant no. 20471003).

References

[1] H. Huppertz, B. von der Eltz, J. Am. Chem. Soc. 124 (2002) 9376.

[2] J.L.C. Rowsell, N.J. Talor, L.F. Nazar, J. Am. Chem. Soc. 124 (2002) 6522.

[3] J. Ju, J.H. Lin, G.B. Li, T. Yang, H.M. Li, F.H. Liao, C.K. Loong, L.P. You, Angew. Chem. Int. Ed. 42 (2003) 5607–5610.

[4] J. Ju, T. Yang, G.B. Li, F.H. Liao, Y.X. Wang, L. P You, J.H. Lin, Chem. Eur. J. 10 (2004) 3901.

[5] T. Yang, G.B. Li, L.P. You, J. Ju, F.H. Liao, J.H. Lin, Chem. Commun. (2005) 4225–4227.

[6] C. Chen, Y. Wang, B. Wu, K. Wu, W. Zeng, L. Yu, Nature 373 (1995) 322.

[7] C. Chen, B. Wu, A. Jiang, G. You, Sci. Sin. (China) B 28 (1985) 235.

[8] C. Chen, Y. Wu, A. Jiang, B. Wu, G. You, R. Li, S. Lin, J. Opt. Soc. Am. B 6 (1989) 616.

[9] S.A. Vinogradova, D. Yu. Pushcharovsky, A.V. Arakcheeva, O.V. Dimitrova, Cryst. Rep. 47 (2002) 24–28.

[10] O. Ferro, S. Merlino, S.A. Vinogradova, D. Yu. Pushcharovsky, O.V. Dimitrova, J. Alloys Compds. 305 (2000) 63–71.

[11] L.Y. Li, X.L. Jin, G.B. Li, Y.X. Wang, F.H. Liao, G.Q. Yao, J.H. Lin, Chem. Mater. 15 (2003) 2253–2260.

[12] Z.T. Yu, Z. Shi, Y.S. Jiang, H.M. Yuan, J.S. Chen, Chem. Mater. 14 (2002) 1314–1318.

[13] L.Y. Li, G.B. Li, Y.X. Wang, F.H. Liao, J.H. Lin, Chem. Mater. 17 (2005) 4174–4180.

[14] L.Y. Li, G.B. Li, Y.X. Wang, F.H. Liao, J.H. Lin, Inorg. Chem. 44 (2005) 8243–8248.

[15] G.M. Wang, Y.Q. Sun, G.Y. Yang, J. Solid State Chem. 178 (2005) 729–735.

[16] W.T.A. Harrison, T.E. Gier, G.D. Stucky, Angew. Chem. Int. Ed. Engl. 32 (1993) 724–726.

[17] M.Z. Visi, C.B. Knobler, J.J. Owen, M.I. Khan, D.M. Schubert, Cryst. Growth Des. 6 (2006) 538–545.

[18] Z.L. Yang, S.H. Yang, G.B. Li, Sh.J. Tian, F.H. Liao, J.H. Lin, Acta Phys.-Chim. Sin. 23 (2007) 285–288.

[19] D.M. Schubert, M.Z. Visi, C.B. Knobler, Inorg. Chem. 39 (2000) 2250–2251.

[20] Z.H. Liu, L.Q. Li, W.J. Zhang, Inorg. Chem. 45 (2006) 1430–1432.

[21] Q. Li, F. Xue, T.C.W. Mak, Inorg. Chem. 38 (1999) 4142–4145.

[22] M. Li, J.Z. Chang, Z.L. Wang, H.Z. Shi, J. Solid State Chem. 179 (2006) 3265–3269.

[23] T. Higashi, ABSCOR, Empirical Absorption Based on Fourier Series Approximation, Rigaku Corporation, Tokyo, 1995.

[24] G.M. Sheldrick, SHELXS97 Program for Solution of Crystal Structures, University of Göttingen, Göttingen, Germany, 1997.

[25] G.M. Sheldrick, SHELXL97 Program for Solution of Crystal Structures, University of Göttingen, Göttingen, Germany, 1997.

[26] A.C. Larson, R.B. von Dreele, Report LAUR 86-748, Los Alamos National Laboratory, 1985.

[27] H.M. Rietveld, J. Appl. Crystallogr. 2 (1969) 65–71.

[28] J. Li, Sh.P. Xia, Sh.Y. Gao, Spectrochim. Acta 51 (1995) 519–532.

[29] J.D. Epping, W. Strojek, H. Eckert, Phys. Chem. Chem. Phys. 7 (2005) 2384–2389.

[30] J.C.C. Chan, M. Bertmer, H. Eckert, J. Am. Chem. Soc. 121 (1999) 5238–5248.

[31] J.C.C. Chan, M. Bertmer, H. Eckert, Chem. Phys. Lett. 292 (1998) 154–160.

[32] C.L. Christ, J.R. Clark, Phys. Chem. Miner. 2 (1977) 59.

[33] G. Heller, Topics in Current Chemistry, vol. 131, Springer, Berlin, 1986.

[34] J.R. Clark, Am. Miner. 49 (1964) 1549–1567.

[35] A.A. Brovkin, N.V. Zayakina, V.S. Brovkina, Kristallografiya 20 (1975) 911–916.

[36] N. Penin, M. Touboul, G. Nowogrocki, J. Alloys Compds. 363 (2004) 104–111.

[37] A. Jiang, S. Lei, Q. Huang, T. Chen, D. Ke, Acta Crystallogr. C 46 (1990) 1999.

[38] Z.H. Liu, L.Q. Li, Cryst. Growth Des. 6 (2006) 1247–1249.

[39] H.H.Y. Sung, M.M. Wu, I.D. Williams, Inorg. Chem. Commun. 3 (2000) 401–404.

[40] C.Y. Pan, G.M. Wang, S.T. Zheng, G.Y. Yang, Z. Anorg. Allg. Chem. 633 (2007) 336–340.

[41] S. Ghose, C. Wan, H.H. Ulbrich, Acta Crystallogr. B 32 (1976) 824–832.

[42] H. Behm, Acta Crystallogr. C 44 (1988) 1348–1351.

[43] S.C. Abrahams, J.L. Bernstein, C. Svensson, J. Chem. Phys. 75 (1981) 1912–1918.

[44] A. Wiesch, K. Bluhm, Z. Naturforsch. 52b (1997) 227–230.

[45] N. Penin, M. Touboul, G. Nowogrocki, Solid State Sci. 5 (2003) 795–803.

[46] R.J. Nelmes, F.R. Thornley, J. Phys. C 7 (1974) 3855–3874.